Journal of Electroceramics, 7, 107–111, 2001

Mixed Electronic-Ionic Conduction in Ru-Doped $SrTiO_3$ at High Temperature

HIROSHIGE MATSUMOTO, DAISUKE MURAKAMI, TETSUO SHIMURA, SHIN-ICHI HASHIMOTO & HIROYASU IWAHARA

Center for Integrated Research in Science and Engineering, Nagoya University, Furo-cho, Chikusa-ku, Nagoya 464-8603, Japan

Submitted January 31, 2001; Revised August 14, 2001; Accepted August 14, 2001

Abstract. The electronic and ionic conduction behavior of Ru-doped $SrTiO_3$ at high temperature was investigated. The conductivity increased significantly with increasing Ru content. $SrTi_{0.80}Ru_{0.20}O_{3-\delta}$ exhibits fairly high conductivities, e.g., 3 S cm^{-1} at 1000°C, and 2 S cm^{-1} at 600°C. The conductivity had only a slight dependence on the partial pressure of oxygen over a wide range and was largely attributed to *n*-type electronic conduction. Ru-doped $SrTiO_3$ showed mixed oxide-ionic and electronic conduction under reducing atmospheres. The mechanism of the electronic and ionic conduction is discussed.

Keywords: $SrTiO_3$, Ruthenium, electronic conduction, ionic conduction

1. Introduction

Mixed electronic and oxide-ionic conductors have received increasing interest given to their potential for application in electrochemical oxygen separators and membrane reactors. The use of such membranes towards the partial oxidation of methane to produce synthetic gas and subsequently for the production of methanol and/or hydrogen has been of particular recent interest. Several kinds of mixed conductors with high oxygen flux have been reported to date, e.g., the perovskites based on the La-Sr-Fe-Co-O system [1], $SrCo_{0.5}FeO_x$ [2], and Fe-doped $LaGaO_3$-based materials [3]. For use in membrane reactors, the material should be tolerant to reducing atmospheres and exhibit good mechanical strength in addition to high electronic and ionic conductivities.

Mixed ionic-electronic conduction in $SrTiO_3$-based compounds at elevated temperature has been reported [3–7]. Iron-doped $SrTiO_3$, in particular, is a mixed conductor of oxide ions and electrons [3–7]. $SrTiO_3$ has the perovskite-type structure and is advantageous due to its mechanical strength and chemical stability. Introduction of electronic and/or ionic conduction to $SrTiO_3$ may be attractive from a practical point of view. On the other hand, $SrRuO_3$ also belongs to the perovskite-type oxides and is known to have a high electronic conduction [8]. It can be assumed that the partial substitution of Ru for Ti may be an effective way to introduce electronic conduction in $SrTiO_3$. In this study, $SrTiO_3$-rich solid solutions between $SrTiO_3$ and $SrRuO_3$ were prepared via the solid state reaction route. Their electronic and ionic properties were investigated at temperatures from 600 to 1000°C.

2. Experimental

Sintered bodies of $SrTi_{1-x}Ru_xO_{3-\delta}$ ($x = 0.05$–0.20) were prepared by solid state reaction. Appropriately weighed amounts of $SrCO_3$, TiO_2 and RuO_2 were mixed and calcined at 1200°C for 10 h in air. The calcined powder was ground, isostatically pressed at 200 MPa and sintered at 1700°C for 10 h in air. Ceramics of black color with relative densities of 94–96% were obtained. Powder X-ray diffraction measurements on the products were performed at room temperature using CuKα radiation.

The electrical conductivity was measured using the complex impedance method from 600 to 1000°C in air and in hydrogen; these gases were saturated with water vapor at room temperature. Porous platinum was used

as the electrodes. The dependence of the conductivity on the partial pressure of oxygen was measured at 800°C. The atmosphere was controlled by using moist O_2–Ar and Ar–H_2 mixtures. The thermoelectric power was semi-quantitatively measured in air at 600–900°C to determine the type of electronic conduction.

The ionic contribution to the conductivity was estimated using gas concentration cells in the reducing and oxidative atmospheres. Using disk-shape samples with porous platinum electrodes, the EMFs of cells (1) and (2) were measured.

$$H_2, Pt|specimen|Pt, H_2 + Ar \qquad \text{cell (1)}$$

$$air, Pt|specmen|Pt, O_2 \qquad \text{cell (2)}$$

The electrochemical self-permeation of hydrogen and oxygen were also measured using the cell (3).

$$H_2 \text{ or } O_2|specimen|Ar \qquad \text{cell (3)}$$

The evolution of hydrogen and oxygen in the outlet of the carrier argon gas with a controlled amount of water vapor was determined by gas chromatography and a zirconia-type oxygen sensor, respectively. The pure and diluted hydrogen gases used in cells (1) and (3) were moistened with water vapor saturated at room temperature. The O_2 and air in cells (2) and (3) were desiccated with a dry ice-ethanol cold trap.

3. Results

3.1. XRD

Figure 1 shows the powder X-ray diffraction patterns of $SrTi_{1-x}Ru_xO_{3-\delta}$ ($x = 0.05$–0.20). All of the specimens examined are single-phase with the cubic perovskite-type structure. The lattice constant, included in the figure, increases almost linearly with increasing amount of Ru dopant. The expansion of the lattice constant is due to the increase in the ionic size from Ti to Ru; the ionic radii of Ti^{4+} and Ru^{4+} with six-fold coordination are 60.5 pm and 62 pm, respectively [9].

3.2. Electrical Conductivity

The electrical conductivities of $SrTi_{1-x}Ru_xO_{3-\delta}$ ($x = 0.05$–0.20) measured in moist air and hydrogen are plotted versus reciprocal temperature in Fig. 2. In both atmospheres, the conductivity increases significantly with increasing Ru dopant content. High

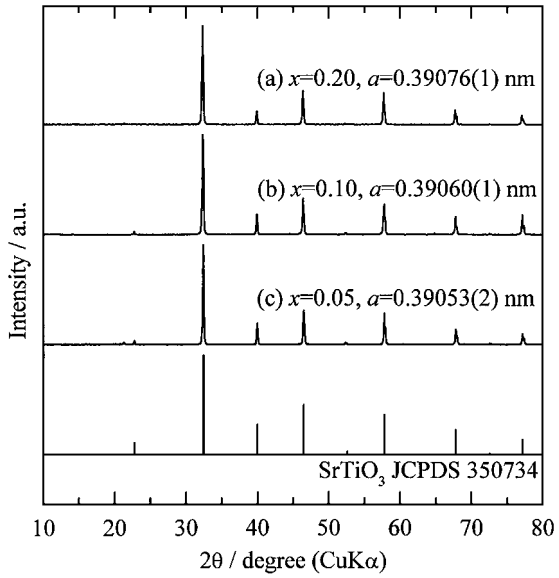

Fig. 1. Powder X-ray diffraction patterns of $SrTi_{1-x}Ru_xO_{3-\delta}$ ($x = 0.05$–0.20) together with lattice constants of cubic unit cells: (a) $SrTi_{0.80}Ru_{0.20}O_{3-\delta}$, (b) $SrTi_{0.90}Ru_{0.10}O_{3-\delta}$, (c) $SrTi_{0.95}Ru_{0.05}O_{3-\delta}$.

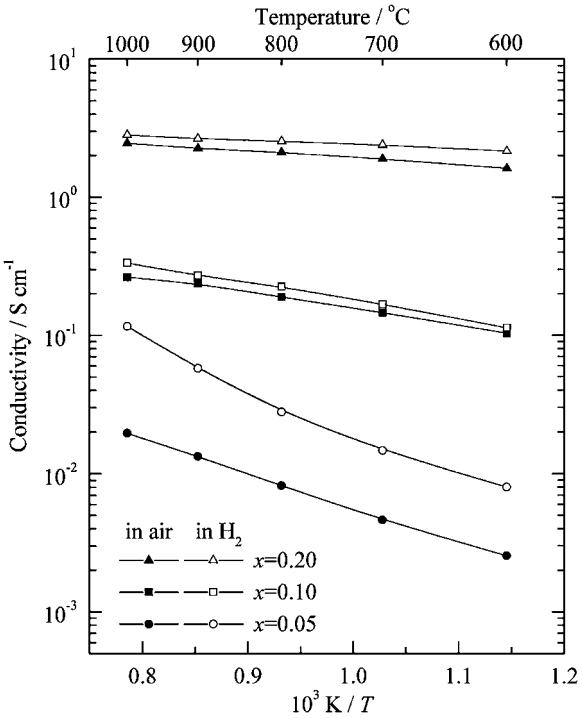

Fig. 2. Temperature dependence of electrical conductivities of $SrTi_{1-x}Ru_xO_{3-\delta}$, $x = 0.05$–0.20, in moist air and hydrogen.

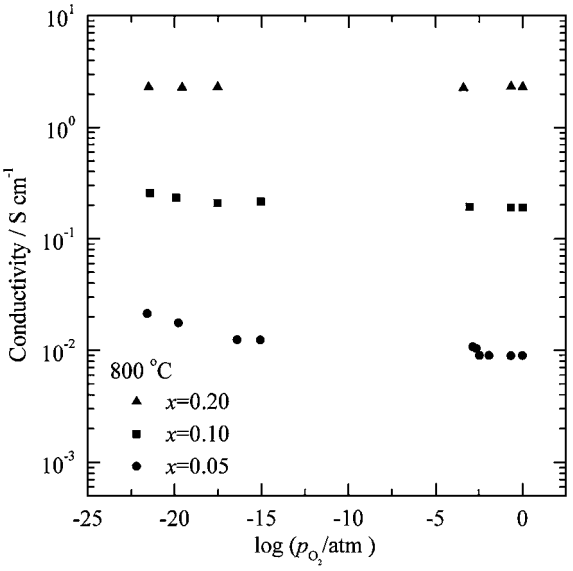

Fig. 3. Dependence of electrical conductivities of $SrTi_{1-x}Ru_xO_{3-\delta}$, $x = 0.05$–0.20, on partial pressure of oxygen at 800°C.

conductivities of about 3 S cm^{-1} at 1000°C and 2 S cm^{-1} at 600°C are observed for the specimen with $x = 0.20$. At the concentration of $x = 0.05$, the conductivities in hydrogen are apparently higher than those in air. At $x = 0.10$ and 0.20, each specimen has almost the same conductivities under the two atmospheres.

The dependence of the conductivity on the partial pressure of oxygen measured at 800°C is shown in Fig. 3. The conductivity has only a slight dependence on p_{O_2}over a wide range. At $x = 0.05$, a slight increase in conductivity, observed in the reducing atmosphere, is consistent with the difference between the conductivities in hydrogen and in air as shown in Fig. 2.

3.3. Electrochemical and Thermoelectric Properties

Figure 4 shows the EMF observed for the cell (1) at 800°C. The dashed line indicates 1/100 of the theoretical EMF calculated from the Nernst equation:

$$E_{\text{Theo}} = \frac{RT}{2F} \ln \frac{p_{H_2,I}}{p_{H_2,II}}. \quad (4)$$

Since the water vapor pressures in the two electrode compartments were the same, the equation would hold both for oxide-ionic and protonic conductors. Very small EMFs, at most, about 1/100 of the theoretical value ($x = 0.05$), were obtained. The measured EMFs

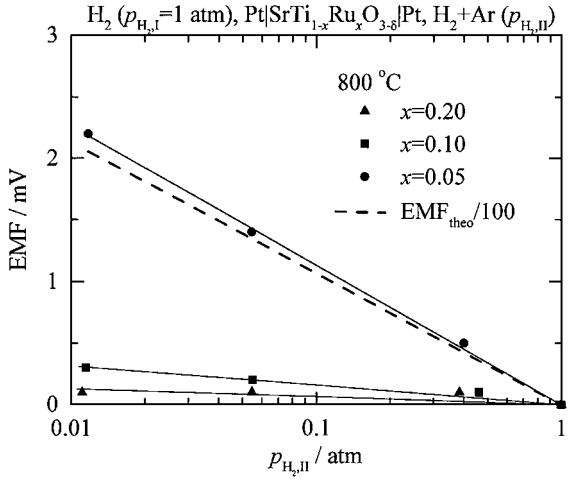

Fig. 4. EMF of the cell: H_2, Pt| $SrTi_{1-x}Ru_xO_{3-\delta}$|Pt, H_2 + Ar ($x = 0.05$–0.20), measured at 800°C; the dashed line indicates 1/100 of the theoretical EMF calculated from the Nernst equation.

for cell (2) at 600–1000°C (with the theoretical voltages of 30–42 mV) were very low and difficult to measure accurately. Therefore, the conductivities shown in Figs. 2 and 3 appear to be largely electronic.

Seebeck coefficients of $SrTi_{1-x}Ru_xO_{3-\delta}$ ($x = 0.05$–0.20) measured in air from 600 to 900°C were negative suggesting that the *n*-type charge carrier governs the conductivity.

The permeation rate of hydrogen from the moist 100% hydrogen to the counter sweep gas through $SrTi_{0.90}Ru_{0.10}O_{3-\delta}$ are shown in Fig. 5. There is a

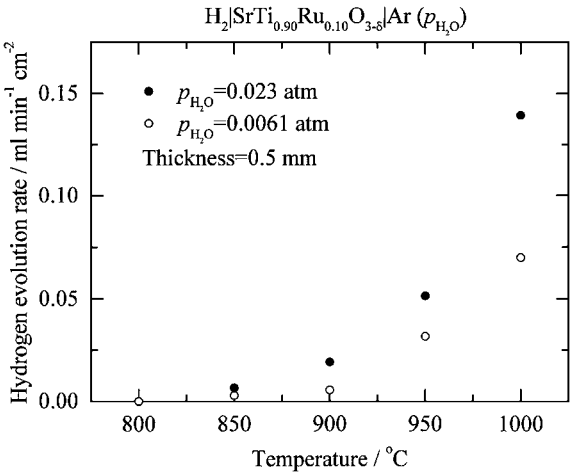

Fig. 5. Evolution rate of hydrogen in Ar carrier gas for $H_2|SrTi_{0.90}Ru_{0.10}O_{3-\delta}|$Ar atmosphere with different water vapor pressures in the carrier gas.

measurable permeation of hydrogen, and the evolution rate of hydrogen increases as the operating temperature and the water vapor pressure in the counter carrier gas increase. When the oxygen permeation was conducted on the same specimen, no evolution of oxygen was experimentally detected in the outlet gas.

4. Discussion

4.1. Electronic Conduction

The conductivity of Ru-doped $SrTiO_3$ significantly increases with the Ru content as shown in Fig. 2, and is almost independent of p_{O_2} as represented in Fig. 3. According to the electrochemical and thermoelectric measurement results, almost all the conduction is based on *n*-type electronic charge carriers.

The p_{O_2}-independent behavior of the electronic conductivity is remarkably different from those of other $SrTiO_3$-based materials. Either pure or doped $SrTiO_3$ generally shows p_{O_2}-dependent electronic conduction at high temperatures [7, 10, 11]. Undoped $SrTiO_3$ has *n*-type conduction over a wide range of p_{O_2} as well as *p*-type conduction near $p_{O_2} = 1$ atm [10, 11]. The *n*-type charge carriers are formed by the following defect equilibrium,

$$Ti_{Ti}^{\times} + 1/2O_O^{\times} \longleftrightarrow Ti_{Ti}' + 1/2V_O^{\bullet\bullet} + 1/4O_2. \quad (5)$$

The conductivities of $SrTi_{0.95}Ru_{0.05}O_{3-\delta}$ ($x = 0.05$) were roughly at the same level as those of undoped $SrTiO_3$ in the low p_{O_2} region. Its negative slope in conductivity observed in Fig. 3 may be ascribed to the reduction of Ti shown in Eq. (5). On the other hand, the conductivities obtained at $x = 0.10$ and 0.20 are much higher than those of pure $SrTiO_3$. Thus, the p_{O_2}-independent conductivity of Ru-doped $SrTiO_3$ is due to Ru doping.

Ru can have three valence states in the six-coordination state: Ru^{3+}, Ru^{4+} and Ru^{5+} [8, 12, 13]. As discussed later, Ru and Ti in the Ru-doped $SrTiO_3$ would have an average valence of nearly 4. The following reaction can be assumed to occur locally around Ru,

$$Ti^{4+} + Ru^{4+} \longleftrightarrow Ti^{3+} + Ru^{5+}. \quad (6)$$

The reaction represents the donation of an electron from the 4*d* orbital of Ru^{4+} to the empty 3*d* orbital of Ti^{4+}. The donated electron is mobile through the Ti 3*d*-like conduction band, contributing to the p_{O_2}-independent *n*-type conduction.

4.2. Ionic Conduction

The electrochemical measurements suggest some ionic contribution in the reducing atmosphere. In the hydrogen permeation experiment, the evolution of hydrogen at the counter compartment was observed and was dependent on the p_{H_2O} in the carrier argon gas. These facts indicate that Ru-doped $SrTiO_3$ has oxide-ionic conduction via oxide ion vacancies. When the proton is the charge carrier, the evolution rate should be independent of p_{H_2O}. Accordingly, in this experiment, hydrogen did not actually permeate through but originated from the electrolysis of water vapor in the carrier gas. The energy for the electrolysis of water vapor is compensated by water formation on the hydrogen side. Oxide ion vacancies can be generated by either the reduction of Ru or Ti,

$$M_{Ti}^{\times} + 1/2O_O^{\times} \rightarrow M_{Ti}' + 1/2V_O^{\bullet\bullet} + 1/4O_2 \ (M = \text{Ru or Ti}). \quad (7)$$

The ionic contribution in the reducing atmosphere discussed above is quite low as indicated by the small EMFs of the hydrogen concentration cell, see Fig. 4. Almost no ionic contribution was observed in the oxidative atmospheres. Therefore, there is a relatively small oxide ion vacancy contribution and Ru and Ti have an average valence of nearly 4 in the compounds under both reducing and oxidative atmospheres.

From the present results, Ru-doped $SrTiO_3$ is characterized by a relatively high and p_{O_2}-independent electronic conductivity. The low ionic conductivity may possibly be improved by the co-substitution of a lower valent cation for Ti^{4+}. The present material has high mechanical strength and is stable against reducing atmospheres. In fact, no degradation was observed during many experiments using the various atmospheres described above. Ru-doped $SrTiO_3$, therefore, warrants further examination as a base material for electrochemical and electronic applications.

Acknowledgments

This work was supported by CREST of JST (Japan Science and Technology). Prof. T. Yogo and Ms.

F. Sweetman are acknowledged for reading the manuscript and providing useful comments.

References

1. Y. Teraoka, H.M. Zhang, S. Fukuwara, and N. Yamazoe, *Chem. Lett*, 1743 (1985).
2. U. Balachandran, J.T. Dusek, R.L. Mieville, R.B. Poeppel, M.S. Kleefish, S. Pei, T.P. Kobylinski, C.A. Udovich, and A.C. Bose, *Appl. Catal. A*, **133**, 19 (1995).
3. Y. Tsuruta, T. Todaka, H. Nisiguchi, T. Ishihara, Y. Takita, Electrochem. *Solid-State Lett*., **4**, E13 (2001).
4. J. Maier, G. Schwitzgebel, and H.-J. Hagemann. *J. Solid State Chem*., **58**, 1 (1985).
5. I. Denk, W. Münch, and J. Maier, *J. Am. Ceram. Soc.,* **78**, 3265 (1995).
6. F. Noll, W. Münch, I. Denk, and J. Maier, *Solid State Ionics*, **86–88**, 711 (1996).
7. S. Steinsvik, R. Bugge, J. Gjønnes, J. Taftø, and T. Norby, *J. Phys., Chem*., **58**, 969 (1997).
8. P.B. Allen, H. Berger, O. Chauvet, L. Forro, T. Jarlborg, A. Junod, B. Revaz, and G. Santi, *Phys. Rev. B*, **53**, 4393 (1996).
9. R.D. Shannon, *Acta Crystallogr. A*, **32**, 751 (1976).
10. N.-H. Chan, R.K. Sharam, and D.M. Smyth, *J. Electrochem. Soc*., **128**, 1981 (1981).
11. U. Balachandran and N.G. Eror, *J. Solid State Chem*., **39**, 351 (1981).
12. C. Mallika and O.M. Sreedharan, *J. Less-Common Metals*, **162**, 51 (1990).
13. I.-S. Kim, T. Nakamura, M. Itoh, and Y. Inaguma, *Mat. Res. Bull*., **28**, 1029 (1993).